Supporting Information

The Bimodal Nickel-Binding Site on *Escherichia coli* [NiFe]-Hydrogenase Metallochaperone HypA

Michael J. Lacasse[1], Kelly L. Summers[2], Mozhgan Khorasani-Motlagh[1], Graham N. George[3], Deborah B. Zamble[1,4]*

[1]Department of Chemistry, University of Toronto, Toronto, Ontario, Canada M5S 3H6, [2]Department of Chemistry, University of Saskatchewan, Saskatoon, Saskatchewan, Canada S7N 5C9, [3]Department of Geological Sciences, University of Saskatchewan, Saskatoon, Saskatchewan, Canada S7N 5E2, and [4]Department of Biochemistry, University of Toronto, Toronto, Ontario, Canada M5S 1A8,

Correspondence to Deborah Zamble: dzamble@chem.utoronto.ca

Table S1. Strains

Description	Source
MC4100	Casadaban, 1976 [1]
DPABF	Hube et al, 2002 [2]

Table S2. Plasmids

Description	Source
strA-pBAD18-kan	Chung et al, 2011 [3]
strA-H2Q-pBAD18-kan	Lacasse et al, 2016 [4]
$HypA_{Str}$-pET24b	Chung et al, 2011 [3]
H2Q-$HypA_{Str}$-pET24b	Lacasse et al, 2016 [4]
C2A, C5A, C7A (TM)-HypB-pET24b	Leach et al, 2005 [5]
TM-C166A-HypB-pET24b	This work
NB-HypB-pET24b [C2A, C5A, C7A, C166A, C198T]	This work
strA-E3A-pBAD18-kan	This work
strA-E3D-pBAD18-kan	This work
strA-C38A-pBAD18-kan	This work
strA-C38S-pBAD18-kan	This work
strA-E40A-pBAD18-kan	This work

Table S3. Primers

Description	Source
Primer: C198T Forward Sequence: 5’-GTTGGCAACCTCGTAACCCCGGCCAGCTTCGATCTC-3’	IDT Technologies
Primer: C198T Reverse Sequence: 5’-GAGATCGAAGCTGGCCGGGGTTACGAGGTTGCCAAC-3’	IDT Technologies
Primer: C166A Forward Sequence: 5’-/P/CGGTAAAGGCGCCCATCTTGA-3’	IDT Technologies
Primer: C166A Reverse Sequence: 5’-/P/GTGTTCACCTGAATCGCTGGTGTG-3’	IDT Technologies
Primer: E3A Forward Sequence: 5’-GGAATTCACCATGCACGCAATAACCCTCTGCCAACG-3’	IDT Technologies
Primer: E3A Reverse Sequence: 5’-CGTTGG CAG AGG GTTATT GCG TGCATGGTGAATTCC-3’	IDT Technologies
Primer: E3D Forward Sequence: 5’-GGAATTCACCATGCACGACATAACCCTCTGCCAACG-3’	IDT Technologies
Primer: E3D Reverse Sequence: 5’-CGTTGGCAGAGGGTTATGTCGTGCATGGTGAATTCC-3’	IDT Technologies
Primer: C38A Forward Sequence: 5’-GCTCAAAATTGGCGCATTTTCTGCTGTCGAAACCAGCTCTCTTG-3’	IDT Technologies
Primer: C38A Reverse Sequence: 5’-CAAGAGAGCTGGTTTCGACAGCAGAAAATGCGCCAATTTTGAGC-3’	IDT Technologies
Primer: C38S Forward Sequence: 5’-GCTCAAAATTGGCGCATTTTCTAGCGTCGAAACCAGCTCTCTTG-3’	IDT Technologies
Primer: C38S Reverse Sequence: 5’-CAAGAGAGCTGGTTTCGACGCTAGAAAATGCGCCAATTTTGAGC-3’	IDT Technologies
Primer: E40A Forward Sequence: 5’-GCATTTTCTTGTGTCGCAACCAGCTCTCTTGCC-3’	IDT Technologies
Primer: E40A Reverse Sequence: 5’-GGCAAGAGAGCTGGTTGCGACACAAGAAAATGC-3’	IDT Technologies

Table S4. Ni(II) Bond lengths from DFT calculations

DFT $HypA_{Pep}$ (Å)		DFT $HypA_{Pep}$ with H_2O (Å)	
Term. Amine	1.93	Term. Amine	1.93
Amide (His2)	1.87	Amide (His2)	1.87
Glu3	2.00	H_2O	1.96
His2	1.93	His2	1.92

Table S5. NB-HypB apparent metal dissociation constants

Cofactor	Condition	Kd (μM)[a]		
		Average	±	Standard Deviation
NoN	MF2 Control	1.3	±	0.3
	NB-HypB	10.3	±	0.7
GDP	MF2 Control	2.8	±	0.4
	NB-HypB	>100		
GppCp	MF2 Control	5.2	±	0.7
	NB-HypB	>100		

[a] Apparent dissociation constants were calculated following competition experiments with the indicated fluorescent metal sensing dye and analysis of the data by using DynaFit. Binding models were selected based on the metal stoichiometries of 1:2 metal: protein. The values presented are averages from three experiments ± one standard deviation.

```
[task]
   data = equilibria
   task = fit

[mechanism]
   M + MF2 <==> M.MF2  :  Kd1  dissoc.
   M + HypA <==> M.HypA  :  Kd2  dissoc.
   M + HypB <==> M.HypB  :  Kd3  dissoc.

[concentrations]
MF2 = 1
HypA = 10
HypB = 0

[constants]
  Kd1 = 5.22
  Kd2 = 4.4  ?
  Kd3 = 100

[responses]
  M.MF2 = 1
  MF2 = 0

[equil]
   variable M
   offset auto ?
                        file    ./data/data.txt

[output]
   directory ./DynaFitOutput/

[end]
;=====================================================================
```

Figure S1. Custom DynaFit script

Custom DynaFit script used to calculate the dissociation constants for the competition experiments. The concentrations (µM) and known dissociation constants were adjusted as appropriate.

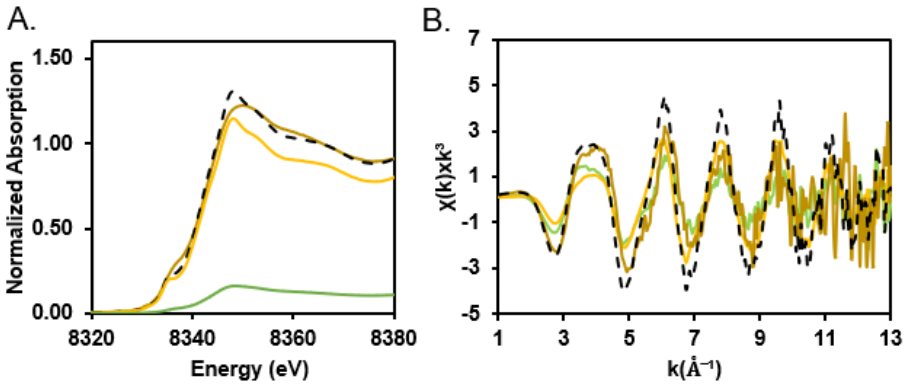

Figure S2. XAS analysis of Ni(II)-HypAStr+TM-HypB(GDP)

(A) Near-edge reconstruction (dashed line) and (B) k^3-weighted EXAFS reconstruction (dashed line) of Ni(II)-HypA$_{Str}$+TM-HypB(GDP) XAS (gold) with 88% Ni(II)-TM-HypB(GDP) (yellow) and 12% Ni(II)-HypA$_{Str}$ (green). The reconstruction is poor indicating that the mixture of the two proteins creates a nickel site distinct from the two separate components.

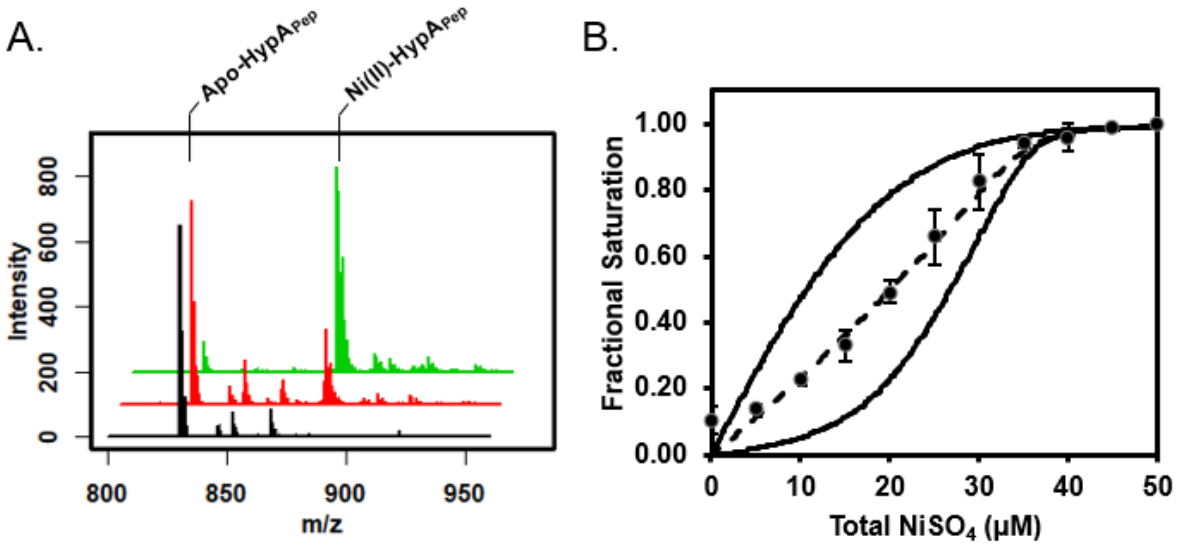

Figure S3. HypA$_{Pep}$ ESI-MS and MF2 - HypA$_{Pep}$ nickel competition

(A) Representative native ESI-MS of 10 μM HypA$_{Pep}$ (black), with 10 μM Ni(II) acetate (red), or 100 μM Ni(II) acetate (green). The intensity of apo-HypA$_{Pep}$ (830 Da) decreases with the addition of Ni(II) and Ni(II)-HypA$_{Pep}$ (889 Da) increases. Only a 1:1 Ni(II)-HypA$_{Pep}$ complex was observed. The Ni(II) complexes have the characteristic isotopic distribution. Small peaks are assigned as salt adducts or impurities. (B) Ni(II) was titrated into a solution containing 20 μM MF2 and 20 μM HypA$_{Pep}$ and changes in the MF2 electronic absorption spectrum [$A_{322\ nm}/(A_{322\ nm} + A_{369\ nm})$] were converted to fractional saturation. Data from four independent experiments were fit, using a custom DynaFit script (Supplemental Figure 1), to an average K_d of 100 ± 30 nM. The fractional saturation of the average dissociation constants (dashed) and fractional saturation from tenfold weaker and tenfold tighter dissociation constants (black) are shown. Data points are the average of four replicates and error bars represent ± one standard deviation.

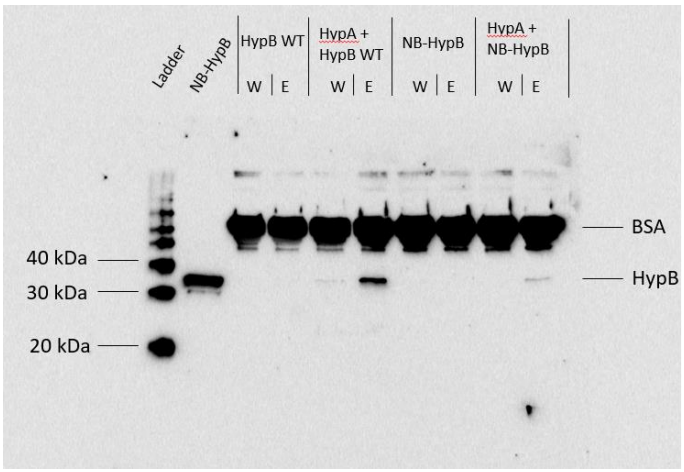

Figure S4. NB-HypB - $HypA_{Str}$ pull down

Lane 1 – Ladder and Lane 2 – NB-HypB (12.5 pg). The remaining lanes are the last wash (W) and elution (E) fractions from experiments with the noted protein mixtures. Proteins were incubated together for 30 min at 4 °C and loaded onto Strep-Tactin resin. The resin was washed with buffer to remove any unbound protein and any bound material was subsequently eluted using the buffer with D-desthiobiotin. The WT-HypB and NB-HypB control experiments demonstrated that HypB was not able to bind to the affinity resin without $HypA_{Str}$. When incubated with $HypA_{Str}$, both WT-HypB and NB-HypB were detected in the elution but not the last wash, indicating coelution and interaction with HypA.

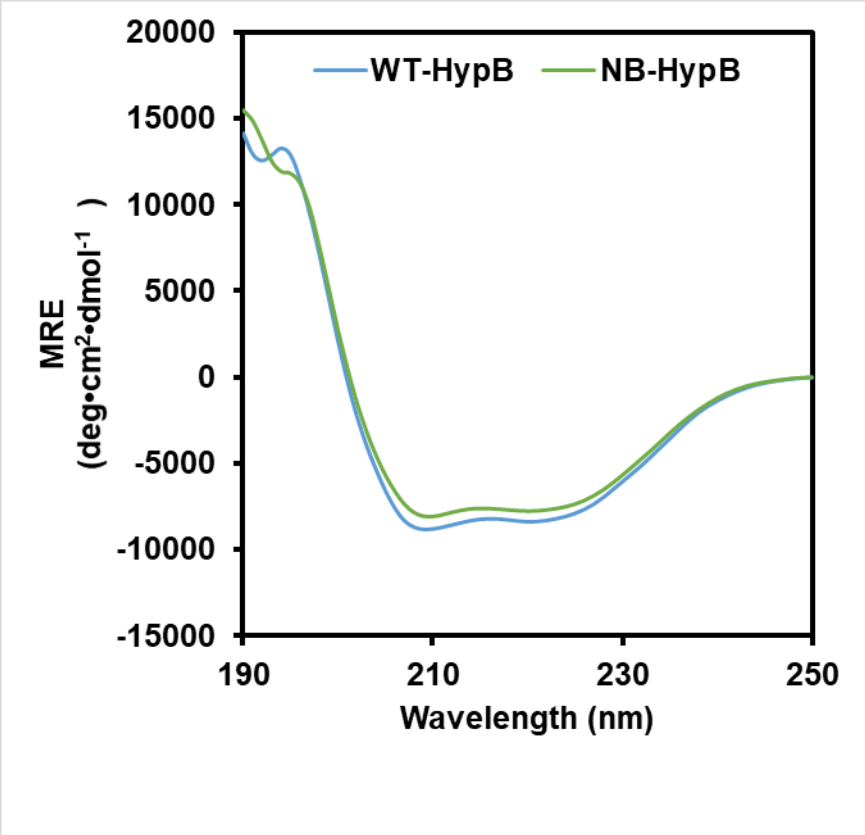

Figure S5. NB-HypB and WT-HypB circular dichroism spectra

WT-HypB and NB-HypB were prepared for CD spectroscopy by buffer exchanging into 100 mM potassium phosphate buffer, pH=7.5, in an anaerobic glovebox (95% N_2, 5% H_2) and diluted to a final concentration of approximately 10 µM. The CD spectra were collected on a Jasco J-710 spectropolarimeter by scanning the wavelength range of 190−250 nm at room temperature. Spectra were collected at 1 nm intervals with a scan speed of 100 nm/min. The final spectra obtained are averages of 10 scans and corrected by subtracting the background buffer signal. The observed ellipticity was converted into mean residue ellipticity.

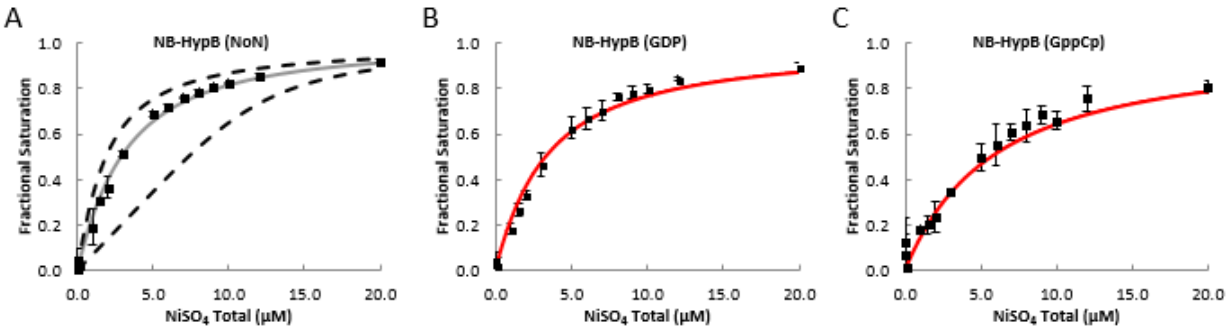

Figure S6. Ni(II) MF2 - NB-HypB competition

Ni(II) was titrated into 1 µM MF2 and 20 µM NB-HypB in the presence of (A) no nucleotide, (B) GDP, and (C) GppCp. The data were fit using a custom DynaFit script (Supplemental Figure 1) to the apparent dissociation constants listed in Supplemental Table 5. The fractional saturation of the average dissociation constants from three independent experiments (dashed) and fractional saturation from tenfold weaker and tenfold tighter dissociation constants (black) are shown. In the event that no competition was observed, as was the case with NB-HypB(GDP) and NB-HypB(GppCp), the MF2 binding curves calculated from the apparent dissociation constants measured in the absence of protein (Supplemental Table 5) are shown in red. Data points are the average of three replicates and error bars represent the standard deviation.

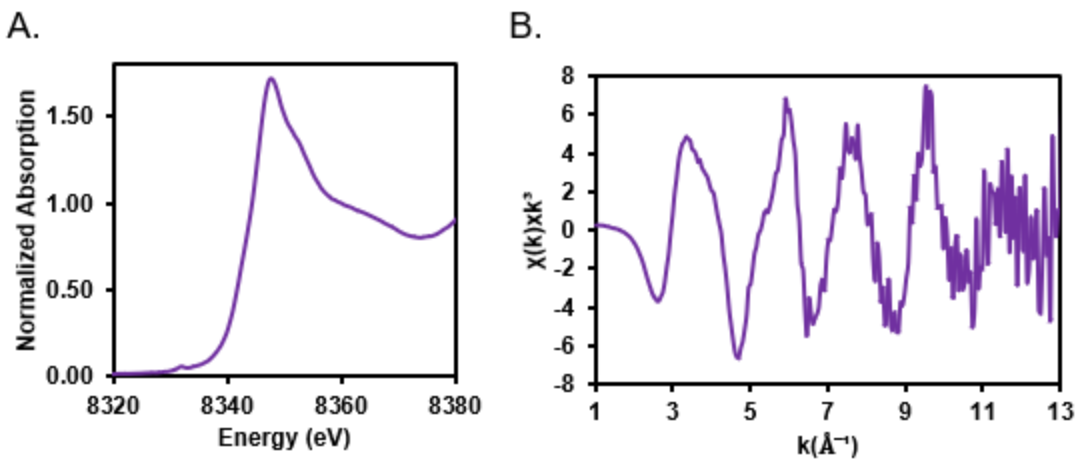

Figure S7. NB-HypB XAS

(A) near-edge and (B) k3-weighted EXAFS of Ni(II) NB-HypB(GDP) (purple). The near-edge spectrum of Ni(II)-NB-HypB has an intense white-line absorbance, consistent with octahedral coordination.

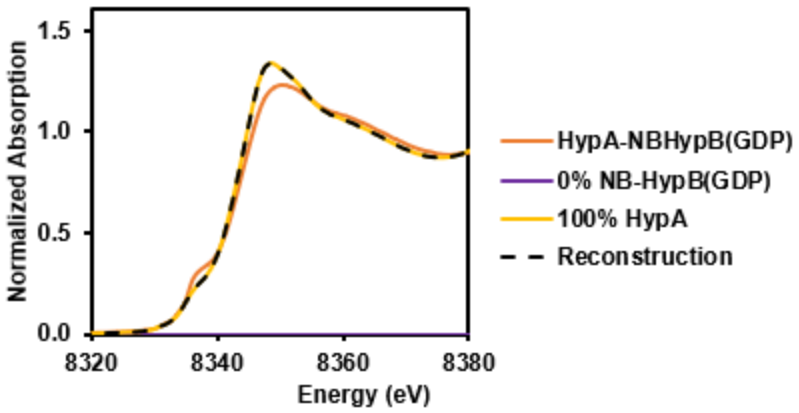

Figure S8. Reconstruction of Ni(II)-HypAStr+NB-HypB(GDP) XAS

(A) Near-edge reconstruction (dashed) of Ni(II)-HypA$_{Str}$+NB-HypB(GDP) XAS (orange) with 0% Ni(II)-NB-HypB(GDP) (purple) and 100% Ni(II)-HypA$_{Str}$ (yellow). The reconstruction fails, indicating that the mixture of the two proteins creates a nickel site distinct from the two separate components.

References

1. Casadaban, M. J. Transposition and fusion of the lac genes to selected promoters in *Escherichia coli* using bacteriophage lambda and Mu. *J. Mol. Biol.* **1976,** 104 (3), 541-55.
2. Hube, M.; Blokesch, M.; Böck, A. Network of hydrogenase maturation in *Escherichia coli*: role of accessory proteins HypA and HypF. *J. Bacteriol.* **2002,** 184 (14), 3879-3885.
3. Chan Chung, K. C.; Zamble, D. B. Protein interactions and localization of the *Escherichia coli* accessory protein HypA during nickel insertion to [NiFe] hydrogenase. *J. Biol. Chem.* **2011,** 286, 43081-43090.
4. Lacasse, M. J.; Douglas, C. D.; Zamble, D. B. Mechanism of selective nickel transfer from HypB to HypA, *Escherichia coli* [NiFe]-hydrogenase accessory proteins. *Biochemistry* **2016,** 55 (49), 6821-6831.
5. Leach, M. R.; Sandal, S.; Sun, H.; Zamble, D. B. The metal-binding activity of the *Escherichia coli* hydrogenase maturation factor HypB. *Biochemistry* **2005,** 44, 12229-12238.